Bioactive Materials 39 (2024) 427–442

Contents lists available at ScienceDirect

Bioactive Materials

journal homepage: www.keaipublishing.com/en/journals/bioactive-materials

Senescence-targeted MicroRNA/Organoid composite hydrogel repair cartilage defect and prevention joint degeneration via improved chondrocyte homeostasis

Ye Sun [a,b,*,1], Yongqing You [c,1], Qiang Wu [b,1], Rui Hu [a], Kerong Dai [b]

[a] Department of Orthopaedics, The First Affiliated Hospital of Nanjing Medical University, Jiangsu, 210029, China
[b] Shanghai Key Laboratory of Orthopaedic Implants, Department of Orthopaedic Surgery, Shanghai Ninth People's Hospital, Shanghai Jiao Tong University School of Medicine, Shanghai, 200011, China
[c] Renal Division, Affiliated Hospital of Nanjing University of Chinese Medicine, Nanjing, China

A B S T R A C T

Introduction: Cartilage defect (CD) is a common complication in osteoarthritis (OA). Impairment of chondrogenesis and cellular senescence are considered as hallmarks of OA development and caused failure of cartilage repair in most clinical CD cases. Exploring markers for cellular senescence in CD patients might provide new perspectives for osteoarthritic CD patients. In the present study, we aim to explore senescent markers in CD patients with OA to fabricate a senescence-targeted SMSC organoid hydrogel for cartilage repair.

Methods: Clinical cartilage samples from cartilage defect patients were collected. Immunofluorescence staining of senescent markers and SA-β-Gal staining were used to detect the senescence state of SMSCs and chondrocytes in cartilage defect and OA patients. MicroRNA expression profiles of SMSC organoids and H2O2-treated SMSC organoids were analyzed and compared with high-throughput microRNA sequencing. Fluorescent in situ hybridization of miRNA were used to determine the expression level of miR-24 in SMSC organoids and cartilage samples. Interaction between miR-24 and its downstream target was analyzed via qRT-PCR, immunofluorescence and luciferase assay. Senescence-targeted miR-24 μS/SMSC organoid hydrogel (MSOH) was constructed for cartilage repair. Anti-senescence properties and chondrogenesis were determined in vitro for MSOH. Rats were used to evaluate the cartilage repair capacity of the MSOH hydrogel in vivo.

Results: In this study, we found Osteoarthritic cartilage defect patients demonstrated upregulated cellular senescence in joint cartilage. MicroRNA sequencing demonstrated senescence marker miR-24 was negatively associated with cartilage impairment and cellular senescence in osteoarthritic CD patients. Moreover, miR-24 mimics alleviates cellular senescence to promote chondrogenesis by targeting downstream TAOK1. Also, miR-24 downregulated TAOK1 expression and promoted chondrogenesis in SMSC organoids. Senescence-targeted miR-24 μS/SMSC organoid hydrogel (MSOH) was constructed and demonstrated superior chondrogenesis in vitro. Animal experiments demonstrated that MSOH hydrogel showed better cartilage repairing effects and better maintained joint function at 24 weeks with low intra-articular inflammatory response after transplantation in rat joint. Single-cell RNA-seq of generated cartilage indicated that implanted MSOH could affect chondrocyte homeostatic state and alter the chondrocyte cluster frequency by regulating cellular glycolysis and OXPHOS, impacting cell cycle and ferroptosis to alleviate cellular senescence and prevent joint degeneration.

Conclusion: Osteoarthritic cartilage defect patients demonstrated upregulated cellular senescence in joint cartilage. Senescence marker miR-24 was negatively associated with cartilage impairment in osteoarthritic CD patients. miR-24 attenuates chondrocytes senescence and promotes chondrogenesis in SMSC organoids through targeting TAOK1. Senescence-targeted miR-24 microsphere/SMSC organoid composite hydrogel could successfully repair cartilage defect in osteoarthritic microenvironment via enhanced miR-24/TAOK1 signaling pathway, suggesting MSOH might be a novel therapy for cartilage repair in osteoarthritic CD patients.

1. Introduction

Degenerative joint disease is the major cause of disability worldwide [1]. Cartilage defects (CD) often complicate with OA and have become an intractable problem in clinical practice for the lack of self-renewing ability due to cellular senescence and impaired chondrogenesis in vivo [2]. Nowadays, clinical options of CD treatment are not satisfying if joint preservation is considered. Osteochondral allograft transplantation is one feasible way to repair damaged cartilage of knee, however, the application is not widely adopted because the source of healthy cartilage is limited, therefore making it unable to restore widespread CD in joint [3]. Besides, high tibial osteotomy and unicompartmental knee

Peer review under responsibility of KeAi Communications Co., Ltd.
* Corresponding author. Department of Orthopaedics, The First Affiliated Hospital of Nanjing Medical University, Jiangsu, 210029, China.
E-mail addresses: sunye881005@163.com, sunye@njmu.edu.cn (Y. Sun).
[1] These authors contributed equally to the manuscript.

https://doi.org/10.1016/j.bioactmat.2024.05.036
Received 1 December 2023; Received in revised form 15 May 2024; Accepted 19 May 2024

arthroplasty are other ways available to retain joints with CD, but such surgeries only delay the process of joint degeneration and cannot reverse impaired cartilage [4,5]. So, it's clinically required to develop other ways to effectively treat CD.

Herein, human synovial mesenchymal stromal cells (SMSCs) provide a solution to achieving cartilage repair, bringing a glimmer of hope for solving the therapeutic dilemma through regenerative strategies [6–9]. SMSCs show huge potential in differentiating into several kinds of cells that compose musculoskeletal system. For example, limited ability of myogenic differentiation of SMSCs was found to lead to muscle regeneration [10]. Moreover, SMSCs have proved osteogenic characteristic of achieving bone regeneration in rat model with cranial defects [11]. Most importantly, intra-articular transplantation of SMSCs for cartilage repair has shown potential in facilitating cartilage regeneration with chondrogenic differentiation capabilities, anti-inflammatory effects, and immunomodulatory properties [12–14]. However, the senescent microenvironment in degenerative OA joint would often undermine the chondrogenic properties of SMSCs and lead to further failure of cartilage repairment [15–17]. Moreover, the regulatory mechanism of senescence in osteoarthritis was rarely known. Targeting cellular senescence to maintain cartilage hemostasis [18] may provide new perspectives and solutions for cartilage defect repair in OA patients [19].

Our lab previously developed a protocol of generating 3D-cultured SMSC organoids with high adaptability and efficacy for treating degenerative joint disease, which exploits modulated miRNA expression in organoid-generated treatment for OA [20]. Therefore, we assumed targeting cellular senescence in OA joint could facilitate cellular differentiation and chondrogenesis in SMSC organoid-based treatment for cartilage repair, providing long-term protection for generated cartilage in the OA joint.

In the present study, we aim to explore senescent markers in CD patients with osteoarthritis to fabricate a senescence-targeted SMSC organoid hydrogel for cartilage repair. We demonstrated the correlation between cellular senescence level and osteoarthritis progression in CD patients. In addition, miR-24, one of many highly enriched miRNAs in SMSC organoids, could serve as a senescent marker in CD patients and inflammatory senescence. Moreover, we evaluated the feasibility of applying senescence-targeted miR-24 microsphere/SMSC organoid composite hydrogel (MSOH) for cartilage repair in osteoarthritic CD. The novelty of our study is to have confirmed that miR-24 is the key target of deterring chondrogenic ageing by miR-24/TAOK1 signaling pathway, and therefore expands understandings of cellular senescence modulated by microRNA μS-wrapped organoid hydrogel for cartilage repair and OA prevention in vivo, showing the potential of targeted and precise therapy aiming to reverse senescent chondrogenesis in OA condition.

2. Results

2.1. Osteoarthritic cartilage defect patients demonstrated upregulated cellular senescence in joint cartilage

We collected cartilage samples from cartilage defect patients (Fig. 1A). Safranin-O staining showed that CD patients had less chondrocytes and cartilage matrix than healthy donors; young CD patients had more severe cartilage degeneration than young healthy donors. Immunohistochemical staining showed that p16 was upregulated in both young and aged CD patients (Fig. 1A). After that, quantitative analysis was used to evaluate p16 positive rate of cartilage sample, and it revealed that cartilage from patients with CD, regardless of age difference, has a significantly higher percentage of p16 positive cells than peer donor group (Fig. 1B). Besides, immunostaining showed that HMGB1 and ACAN was both downregulated in young and aged CD patients. The percentage of HMGB1-positive cells was significantly declined in CD patients, especially in aged CD patients. Aged CD patients had significantly higher OARSI score as well, indicating that cell senescence was involved in the osteoarthritic cartilage defect patients. Then we collected chondrocytes from healthy donors and CD patients, and the cells were cultured to observe the state of cellular senescence and potential of self-renew in vitro. SA-β-Gal staining also confirmed the senescent cells increased in CD patients: the percent of SA-β-Gal positive cells significantly increased in aged CD patients (Fig. 1C). Expression of lipid peroxidation marker 4-HNE, DNA damage marker gamma-H2AX and cellular senescence marker p16 were significantly elevated in CD patients, aged patients particularly (Fig. 1D–F; Supplementary Figure 1). Alcian blue staining showed that chondrocytes from aged CD patients had significantly less stained aera and percent of stained cells, suggesting that chondrocytes from aged CD patients had lowest ability of chondrogenesis (Fig. 1G). In addition, qRT-PCR was further conducted to detect the expression of cell cycle related protein (CDKN1a, CDKN2A) and inflammatory factors (MMP3, IL1β, IL6 and MMP13) and it was found that all these factors in CD group upregulated, remarkably higher in aged CD group (Fig. 1H). These results suggest that cellular senescence may play a key role in cartilage defect, indicating that inhibition of cellular senescence could be a potential therapy for cartilage repair and regeneration.

2.2. Cellular senescence marker miR-24 was negatively associated with cartilage impairment and cellular senescence in osteoarthritic CD patients

To further investigate the underlying mechanism of cellular senescence-mediated chondrogenesis in cartilage defect patients, microRNA expression profiles of SMSC organoids and hydrogen peroxide treated SMSC organoids were analyzed and compared with high-throughput microRNA sequencing (Fig. 2A). The hierarchical cluster indicated that the microRNA cargoes in SMSC organoids were obviously different from microRNA cargoes in hydrogen peroxide treated SMSC organoids. Volcano plot of miRNA expression profiles demonstrated that miR-24 was remarkably downregulated in hydrogen peroxide treated SMSC organoids (Fig. 2B). The expression of miR-24 in different groups was further validated by qRT-PCR, showing that the organoids expressed significantly more miR-24 than SMSC (Fig. 2C). Also, the results confirmed that miR-24 was downregulated under hydrogen peroxide treatment condition, and upregulated with senolytic treatment, indicating its potential in cartilage regeneration and cartilage repair therapy. Fluorescent in situ hybridization (FISH) of miR-24 in different groups also confirmed the phenomenon (Fig. 2D, Supplementary Figure 1). Further investigation of cartilage samples showed that expression level of miR-24 significantly reduced in aged CD patients (Fig. 2E). Also, the miR-24 expression level had negative lineal regression with patients' K-L scores (Fig. 2F). Fluorescent in situ hybridization (FISH) of miR-24 in cartilage samples of healthy donors and OA patients showed percent of miR-24 positive cells decreased significantly in OA patients (Fig. 2G).

2.3. miR-24 alleviates cellular senescence to promote chondrogenesis by targeting downstream TAOK1

To search for the potential target genes of miR-24, we collected all the predicted potential target genes for Venn analysis (Fig. 3A). Moreover, a miRNA-mRNA network using the Cytoscape software was constructed. Based on these results, TAOK1, a positive regulator of TLR4 related inflammatory response pathway, was predicted as a target gene of miR-24 (Fig. 3B). The expression of TAOK1 in different groups was further validated by qRT-PCR, showing that the SMSC organoids with senolytic treatment expressed significantly less TAOK1 (Fig. 3C). Additionally, miR-24 shows a high level of sequence conservation among different species (Fig. 3D). To further confirm the functional interaction between miR-24 and TAOK1, we performed a luciferase report assay analysis (Fig. 3E). Upregulation of miR-24 by miR-24 mimics significantly reduced TAOK1 expression while miR-24 inhibitor significantly increased TAOK1 expression in cultured SMSC and SMSC organoids

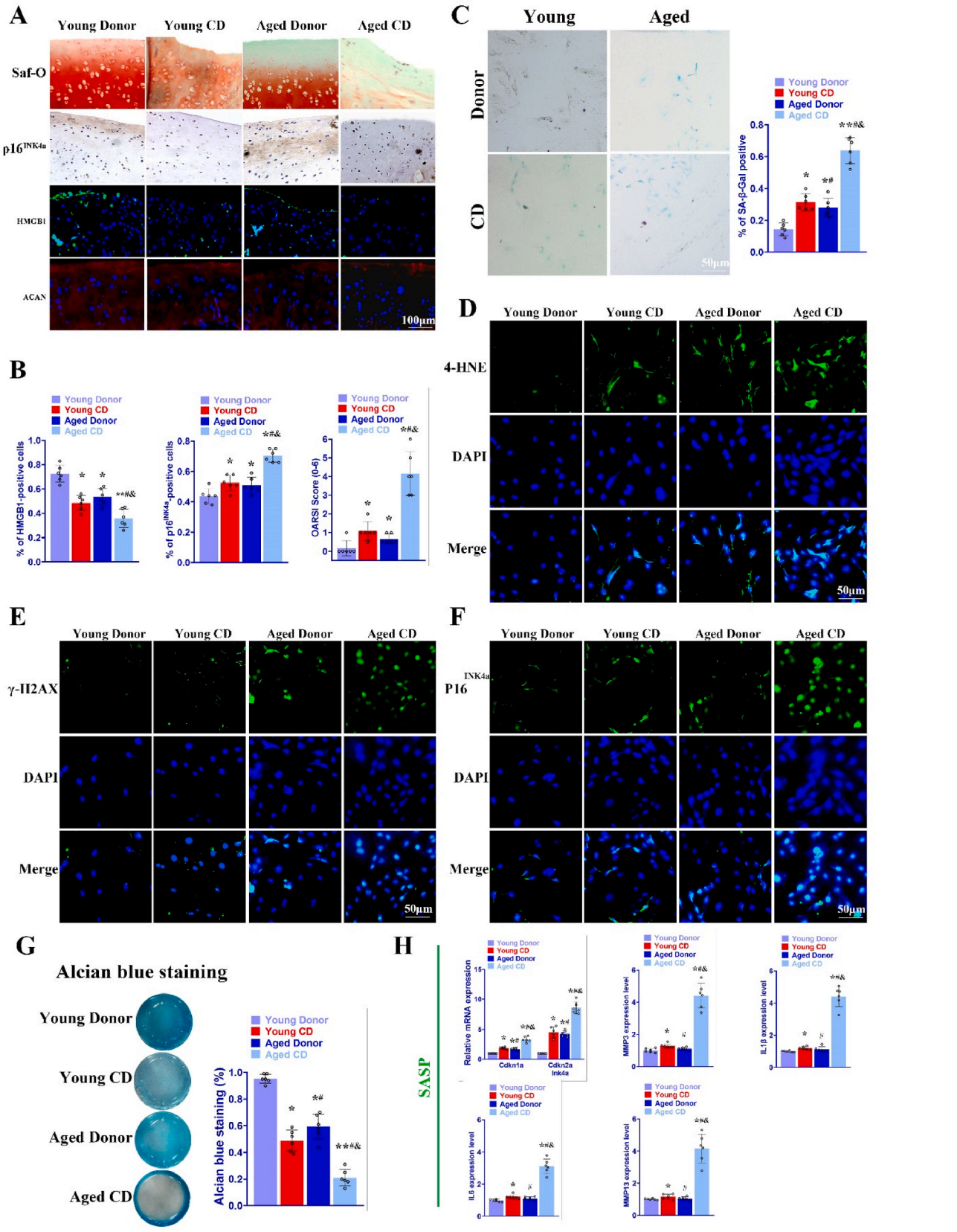

(caption on next page)

Fig. 1. Cellular senescent markers were upregulated in cartilage samples of osteoarthritic cartilage defect patients.
A Safranin-O staining, immunofluorescence staining for $p16^{INK4a}$, HMGB1 and ACAN in cartilage sample from young donor, young CD, aged donor, and aged CD. (green, HMGB1; red, ACAN; blue, DAPI)
B Percent of HMGB1 and $p16^{INK4a}$ positive cell and OARSI score in cartilage sample from young donor, young CD, aged donor, and aged CD. (n = 6 for each)
C SA-β-Gal staining and percent of SA-β-Gal positive cell in cartilage sample from young donor, young CD, aged donor, and aged CD. (n = 6 for each)
D Immunofluorescence staining for 4-HNE and DAPI in cartilage sample from young donor, young CD, aged donor, and aged CD. (green, 4-HNE; blue, DAPI)
E Immunofluorescence staining for γ-H2AX and DAPI in cartilage sample from young donor, young CD, aged donor, and aged CD. (green, γ-H2AX; blue, DAPI)
F Immunofluorescence staining for $p16^{INK4a}$ and DAPI in cartilage sample from young donor, young CD, aged donor, and aged CD. (green, $p16^{INK4a}$; blue, DAPI)
G Alcian blue staining and Alcian blue positive cell in cartilage sample from young donor, young CD, aged donor, and aged CD. (n = 6 for each)
H Relative Cdkn1a, Cdkn2aInk4a, MMP3, IL1β, IL6 and MMP13 expression level in cartilage sample from young donor, young CD, aged donor, and aged CD. (n = 6 for each) *P < 0.05, **P < 0.01 compared to the Young Donor group, #p < 0.05 compared to the Young CD group, &P < 0.05 compared to the Aged Donor group.

(Fig. 3F and G). KEGG pathway analysis based on the differentially expressed genes was conducted and showed closely associated with Hippo signaling pathway, cellular senescence, pathway in cancer, microRNA in cancer and apoptosis (Fig. 3H). Next, we analyzed the biological effects of miR-24 expression on chondrogenesis markers, senescence markers, inflammatory markers, and cell adhesion markers by qRT-PCR (Fig. 3I). The expression of chondrogenesis markers and cell adhesion markers was increased in cultured SMSC and SMSC organoids transfected with miR-24 mimics and TAOK1 siRNA. In contrast, overexpression of miR-24 and inhibition of TAOK1 strongly decreased level of senescence and inflammatory markers, whereas inhibition of miR-24 increased level of cellular senescence and inflammatory markers in SMSC and SMSC organoids. The expression of senescence and inflammatory markers was increased in cultured SMSC and SMSC organoids transfected with miR-24 inhibitor as well. Collectively, the data validated TAOK1 as a direct target of miR-24, and upregulation of miR-24 promotes the chondrogenesis of SMSC and SMSC organoids.

2.4. miR-24 regulates chondrogenesis and prevented cellular senescence of SMSC organoids in vitro

3D-cultured SMSC organoids were generated, transfected with miR-24 mimics, and phenotypically analyzed for potential applications in cartilage defect treatment and chondrogenesis (Fig. 4A). The 3D-cultured SMSC organoids with hydrogen peroxide treatment were produced and analyzed for simulation of cartilage degeneration. MiR-24 mimics transfected SMSCs self-assembled to form a stack of cells to attain a spheroid shape in the 4-week cultivation, demonstrating compaction of the organoids with a confined anti senescence ability (Fig. 4B). Meanwhile, the hydrogen peroxide treated SMSC organoids failed to attain a spheroid shape, expressing abundant senescence markers. Also, 2D-cultured SMSCs were set, showing less anti senescence ability than 3D-cultured SMSC organoids (Fig. 4C). Chondrogenesis was defined for the transfected organoids, showing significantly greater expression of chondrogenic markers SRY-related high mobility group-box gene 9 (SOX9) and aggrecan (ACAN) compared to the 2D cultured groups (Fig. 4D and E). We chose to evaluate senescence, chondrogenesis, inflammatory and cell adhesion in different groups of SMSC and SMSC organoids with qRT-PCR (Fig. 4F). miR-24 mimics transfection decreased cellular senescence and inflammatory compared to the hydrogen peroxide treatment group. Meanwhile, miR-24 mimics transfection not only enhanced chondrogenesis by elevating the expression of chondrogenesis-related genes, but cell adhesion as well. Furthermore, the qPCR profiles confirmed that SMSC organoids significantly greater expression of chondrogenic and cell adhesion markers than the 2D cultured groups under same condition. Examination of ability of chondrogenesis in different treatment of SMSC and SMSC organoids was conducted with enzyme linked immunosorbent assay of GAG, collagen I and II (Fig. 4G). Compared to SMSC groups, SMSC organoids groups showed significantly better ability of chondrogenesis. The concentration of GAG, COL I and COL II in SMSC organoids groups was higher than SMSC groups with same treatment. Also, miR-24 mimics transfection significantly elevated the concentration of GAG, COL I and COL II, indicating that miR-24 mimics promotes chondrogenesis in vitro.

2.5. Fabrication and characterization of MSOH for cartilage repair

miR-24 PLGA μS/SMSC organoid hydrogel (MSOH) was constructed for cartilage repair in rat knee (Supplementary Table 1). Human donors' SMSCs were derived for cell delivery in hydrogel. Cell carrier hydrogel was produced with a mixture of gelatin, fibrinogen, hyaluronic acid and glycerol. Gelatin was used for its thermo-sensitive properties (liquid above 37 °C and solid below 25 °C) in fabrication (Fig. 5A). Before transplanting into the defect site, MSOH hydrogel was crosslinked by a mixture of gelatin, fibrinogen, hyaluronic acid and glycerol to maintain its shape fidelity (Fig. 5B). miR-24 PLGA μs were successfully embedded in the hydrogel. The crosslinked hydrogel showed good shape fidelity with delicate and orderly alignment under light microscope. Scanning electron microscope (SEM) images of most miR-24 PLGA μs demonstrated a less than 5 μm diameter, indicating the uniformity of the PLGA nanoparticle sizes. (Fig. 5B). Size was determined for each PLGA nanoparticle formulation and mean sizes were found to be between 2 μm and 3 μm (Supplementary Figure 2), which is the optimal size for cellular uptake. Dynamic mechanical analysis was performed for composite hydrogel, storage modulus G′ and the loss modulus G″ are presented, exhibiting evident plateau in the frequency range investigated (Fig. 5C and D). Obtained hydrogel showed high G′ value at low temperature, but the storage and loss modulus decreased on heating with a crossover of G″ and G' at temperature of 35 °C. This temperature indicates the transition from an elastic network formation to a solution for the gel. Degradation rate of the composite hydrogel was explored in vitro and in vivo in nude mice (Fig. 5E). The composite hydrogel showed close to 50 % degradation at 2 weeks and a nearly 60 % degradation over 3-weeks after implantation (Fig. 5E). Confocal microscopy demonstrated the SMSC displayed good distribution and coverage of organoid-derived cells in the hydrogel (Fig. 5F). Immunostaining also showed the MSOH hydrogel demonstrated good chondrogenesis with highly expressed ACAN (Fig. 5G).

2.6. Cartilage defect repaired by MSOH transplantation in vivo

Rats were used to evaluate the cartilage repair capacity of the MSOH hydrogel. As shown, full-thickness cartilage defect was created in the rat knee (Fig. 6A). The hydrogel was implanted into the defect site to test for cartilage tissue regeneration. Cartilage repair with MSOH hydrogel showed much better gross appearance than control hydrogel with only gel or SMSC organoids. At 24 weeks, H&E staining showed the integrity of formed neo cartilage tissue. Neo cartilage in the MSOH hydrogel group showed more similar appearance to normal cartilage than the control groups. Histological analysis with safranin-O was used to evaluate generated cartilage by the hydrogel compared to native cartilage. As shown in figure, when the defect was treated with the MSOH hydrogel, fully hyaline-like cartilage was regenerated, as evidence by safranin-O, and better cell filling in H&E staining. Immunostaining of collagen II and ACAN was conducted in the generated cartilage tissue sections in different groups. Compared to the control group, stronger intensity in COL II and ACAN staining, which resembles the native

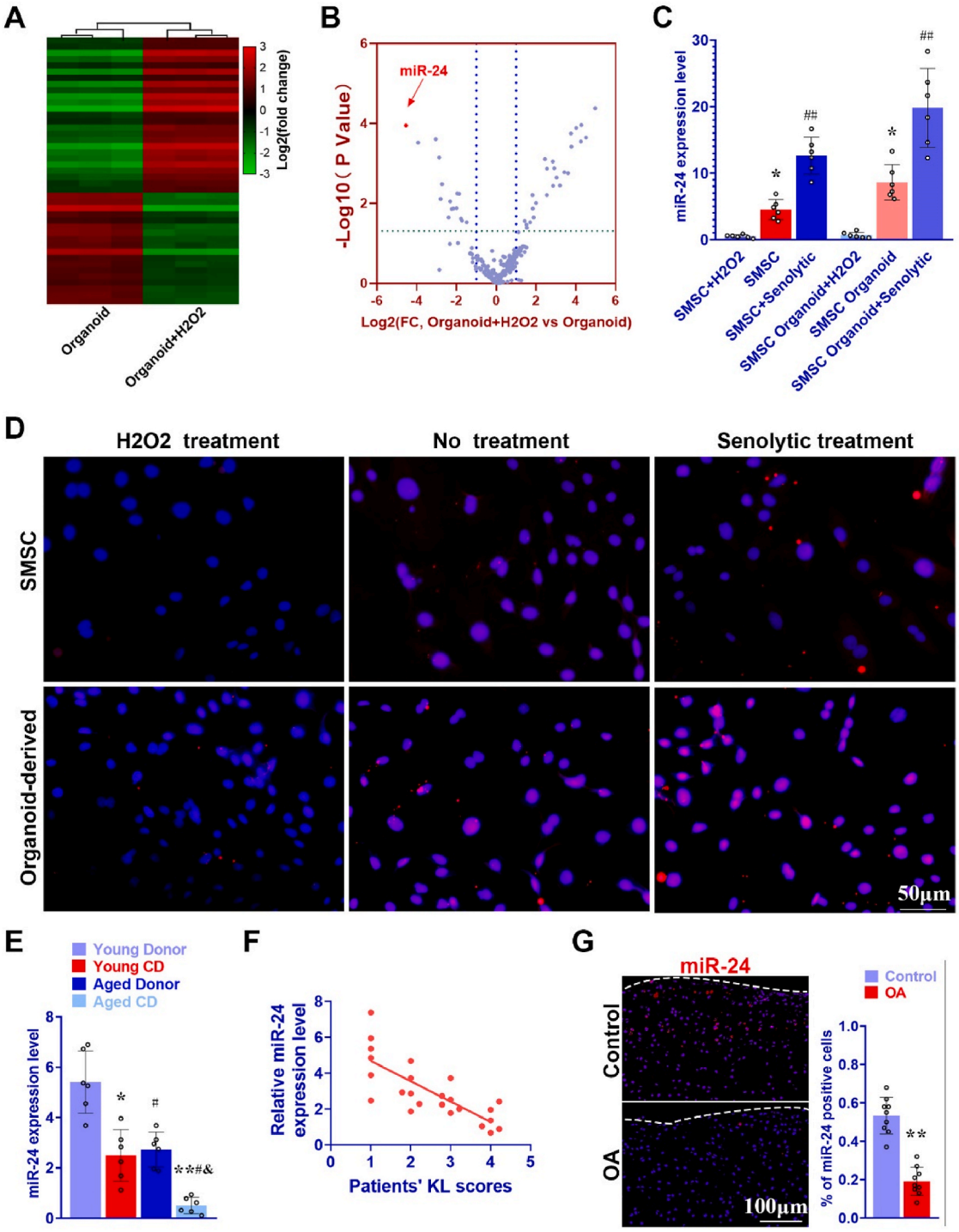

Fig. 2. Discovery of H2O2 treated SMSC organoids-associated miRNAs by microarray and FISH.

A Heatmap of clustering gene expression profiles with microarray in SMSC organoids compared to hydrogen peroxide treated SMSC organoids. (n = 3 for each group)

B Volcano plot of RNA expression profiles of SMSC organoids and hydrogen peroxide treated SMSC organoids. MiR-24 was significantly downregulated in hydrogen peroxide treated SMSC organoids.

C Relative miR24 expression level in SMSC, SMSC + H2O2 treatment, SMSC + senolytics treatment, SMSC organoids, SMSC organoids + H2O2 treatment, SMSC + senolytics treatment. (n = 6 for each) *P < 0.05 compared to the first column group, #p < 0.05, ##p < 0.01 compared to the 2nd column group.

D fluorescent in situ hybridization (FISH) of miR-24 in SMSC, SMSC + H2O2 treatment, SMSC + senolytics treatment, SMSC organoids, SMSC organoids + H2O2 treatment, SMSC + senolytics treatment.

E Relative miR-24 expression level in cartilage sample of young donor, young CD, aged donor, and aged CD. (n = 6 for each) *P < 0.05, **P < 0.01 compared to the Young Donor group, #P < 0.05 compared to the Young CD group, &P < 0.05 compared to the Aged Donor group.

F Relationship between cartilage damage severity and miR-24 expression with linear regression of patients' Kellgren-Lawrence score and relative miR-24 expression level.

G FISH of miR-24 in cartilage sample of OA patients and normal patients, and percent of miR-24 positive cell. (n = 6 for each) **P < 0.01 compared to the Control group.

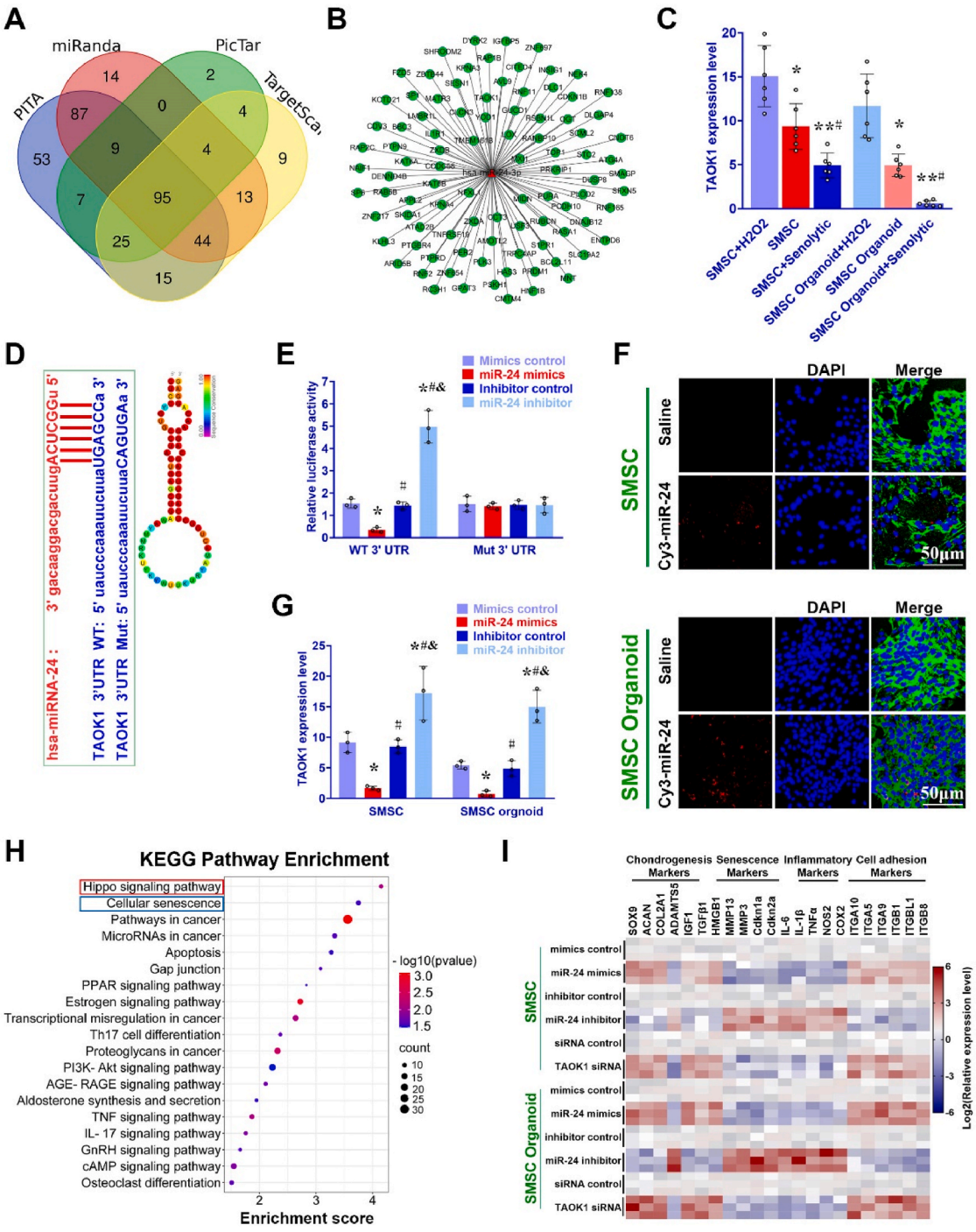

Fig. 3. TAOK1 is a direct target of miR-24 to modulate chondrogenesis.

A Predicted genes were compiled for Venn analysis to search for potential targets of miR-24.

B miRNA-mRNA network using the Cytospace software was constructed for miR-24.

C Relative TAOK1 expression level in SMSC, SMSC + H2O2 treatment, SMSC + senolytics treatment, SMSC organoids, SMSC organoids + H2O2 treatment, SMSC + senolytics treatment. (n = 6 for each) *p < 0.05,**p < 0.01 compared to the first column group, #p < 0.05 compared to the 2nd column group.

D Sequence of wide-type (WT) and mutant (Mut) TAOK1 binding sites for miR-24 (left) and conservation level of miR-24 sequence among species (right).

E Luciferase reporter assay analysis results (n = 3 for each) to confirm the direct interaction between miR-24 and TAOK1 binding sites. *P < 0.05 compared to the mimics control group, #p < 0.05 compared to the miR-24 mimics group, &P < 0.05 compared to the inhibitor control group.

F Fluorescence micrograph of Cy3 (red)-labeled miR-24 mimic internalized by GFP(green)-labeled SMSCs and SMSC organoids.

G relative TAOK1 expression with qRT-PCR in SMSCs and SMSC organoids transfected with miR-24 mimics or inhibitor. (n = 3 for each) *P < 0.05 compared to the mimics control group, #p < 0.05 compared to the miR-24 mimics group, &P < 0.05 compared to the inhibitor control group.

H Significantly enriched pathways for target genes of miRNAs enriched within SMSC in Kyoto Encyclopedia of Genes and Genomes (KEGG) pathways.

I Heatmap of clustering gene expression profiles with q-PCR in SMSCs and SMSC organoids transfected with miR-24 mimics or inhibitor and TAOK1 siRNA. (n = 3 for each).

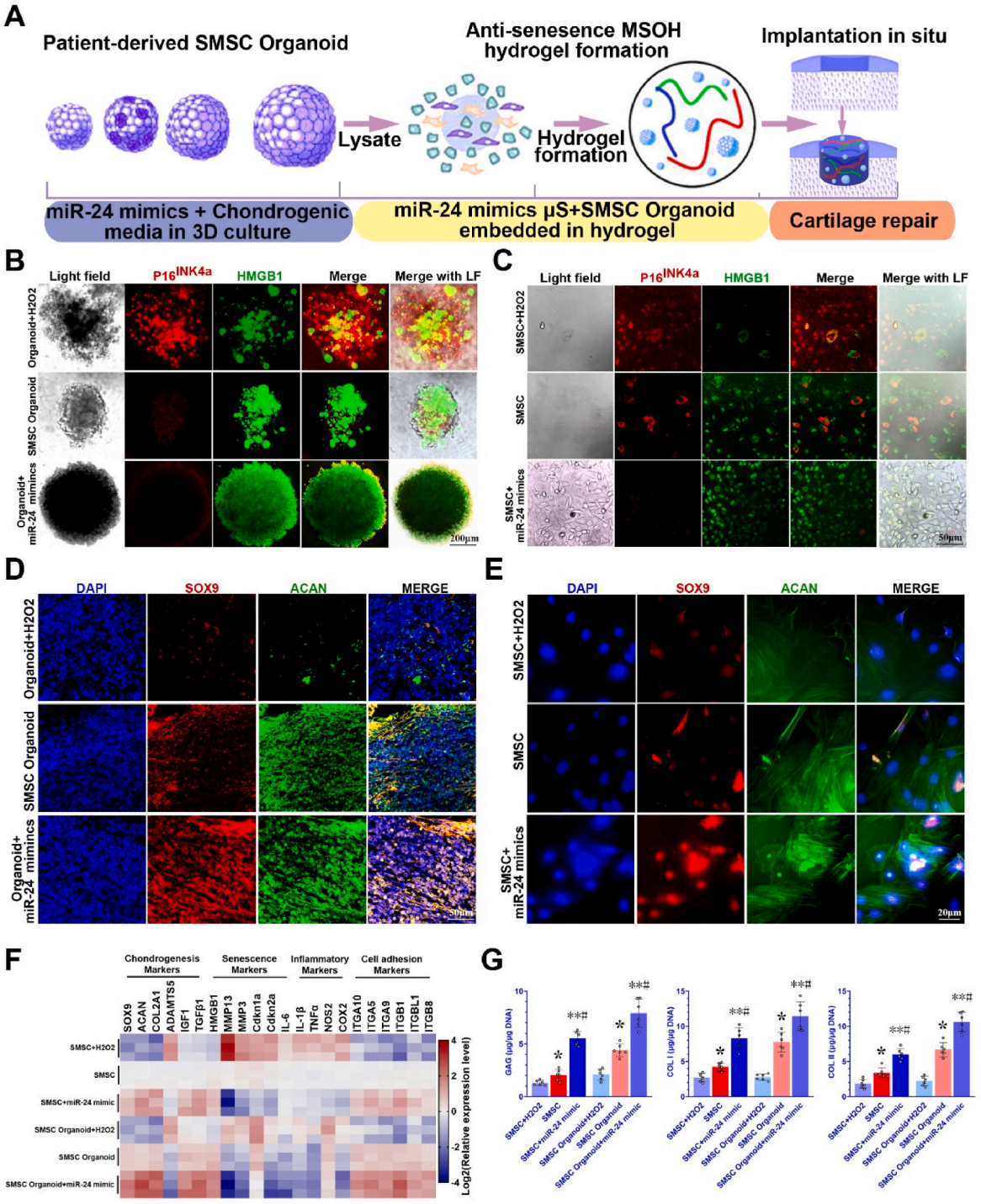

Fig. 4. Generating miR-24 transfected SMSC organoids for anti-senescence and pro-chondrogenesis.
A Fabrication of senescence-targeted miR-24 μS/SMSC organoid hydrogel for potential applications in chondrogenesis and further cartilage repair treatment.
B SMSCs self-assembled to attain a spheroid shape in the four-week cultivation in the SMSC organoids. Immunofluorescence staining of $p16^{INK4a}$ (red) and HMGB1 (green) in SMSC organoids, SMSC organoids + H2O2 treatment and SMSC organoids + miR-24 transfection after 4 weeks.
C 2D cultivation of SMSC. Immunofluorescence staining of $p16^{INK4a}$ (red) and HMGB1 (green) in SMSC, SMSC + H2O2 treatment and SMSC + miR-24 transfection.
D Immunofluorescence staining of chondrogenic marker SOX9 (red) and ACAN (green) in SMSC organoids, SMSC organoids + H2O2 treatment and SMSC organoids + miR-24 transfection.
E Immunofluorescence staining of chondrogenic marker SOX9 (red) and ACAN (green) in SMSC, SMSC + H2O2 treatment and SMSC + miR-24 transfection.
F Heatmap of clustering gene expression profiles with q-PCR in SMSCs and SMSC organoids transfected with miR-24 mimics and H2O2 treatment. (n = 3 for each)
G Quantification of deposited GAGs, collagen I and collagen II in SMSCs and SMSC organoids transfected with miR-24 mimics and H2O2 treatment. (n = 6 for each)
*$p < 0.05$,**$p < 0.01$ compared to the first column group, #$p < 0.05$ compared to the 2nd column group.

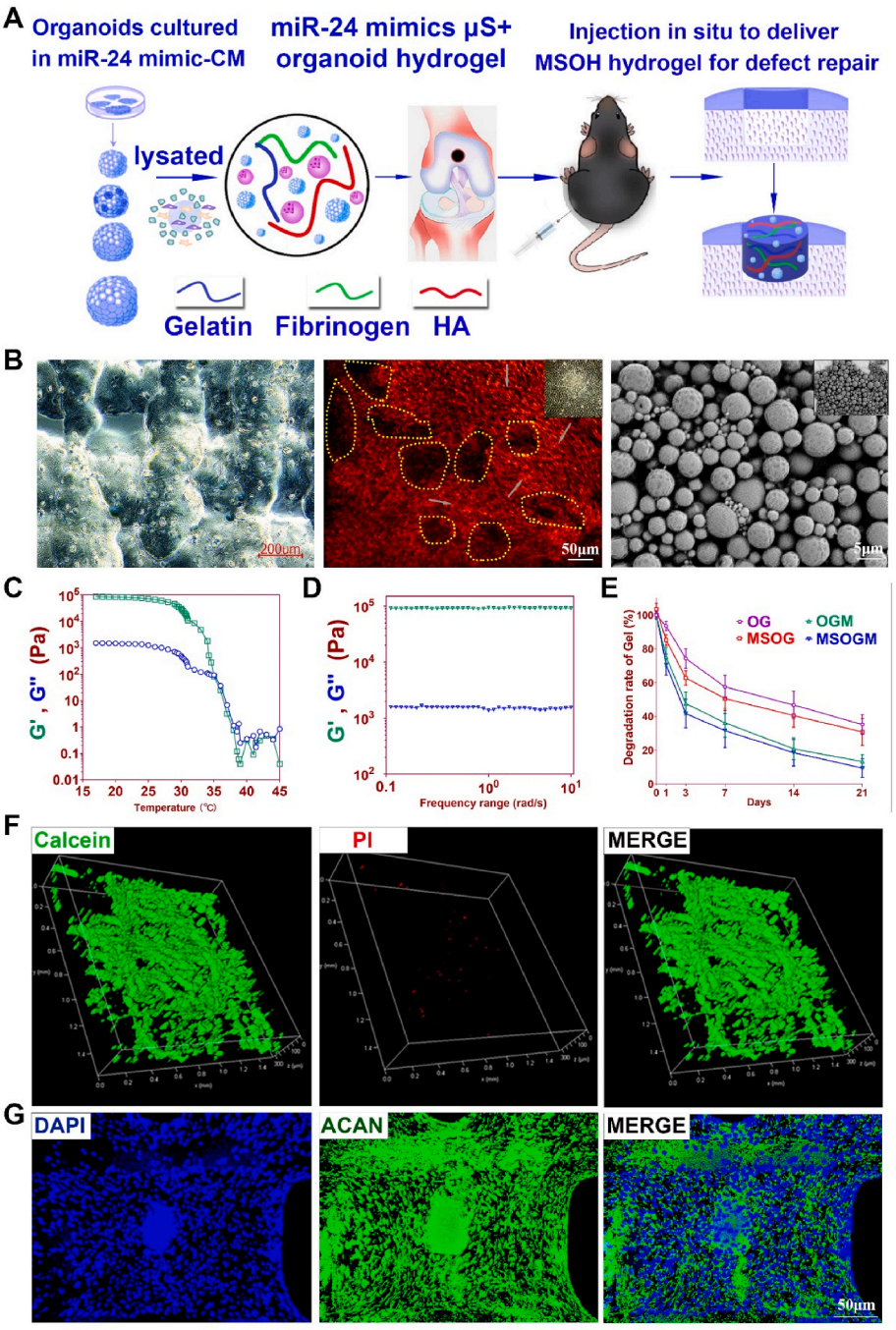

Fig. 5. Characterization of senescence-targeted MSOH hydrogel for cartilage repair in vitro.
A Schematic illustration of the study design with 3D cultured SMSC organoids for cartilage damage treatment by intra-articular injection in rat.
B before transplantation, miR-24 hydrogel was cross-linked by the addition of thrombin to further maintain the shape fidelity of the hydrogel. (left) The cross-linked hydrogel demonstrated good shape fidelity and (medium, right) good distribution of organoids. Organoids were indicated with yellow dotted circles, and organoid was embedded in the hydrogel indicated with grey arrows. (medium: higher resolution image of the partial area in the left image; right: SEM images of miR-24-conjugated hydrogel μs.)
C Dynamic thermal rheological observations of the cross-linkage of MSOH. The temperature dependence of the storage and loss modulus was determined by oscillatory shear deformation with temperature ranging from 15 to 45 °C (heating rate 1.45 °C min-1) at constant frequency (1 Hz) and constant shear strain (γ = 0.05, 1.88 mrad).
D Mechanical spectra of different component and cross-linked hydrogel measure at 17 °C. Storage and loss modulus were recorded in a constant strain mode with a deformation of 0.05 maintained over the frequency range of 0.01–10 Hz (rad/s) at 17 °C
E Degeneration rate of organoid-laden hydrogel in vitro and in vivo.
F 3D-reconstructed images of organoid-laden hydrogel, showing good cell viability with live/dead assay using Calcein-AM/PI double staining kit (green, live cells; red, dead cells) under a confocal microscope.
G Immunofluorescence staining chondrogenic marker gene ACAN (green) in organoid-laden hydrogel.

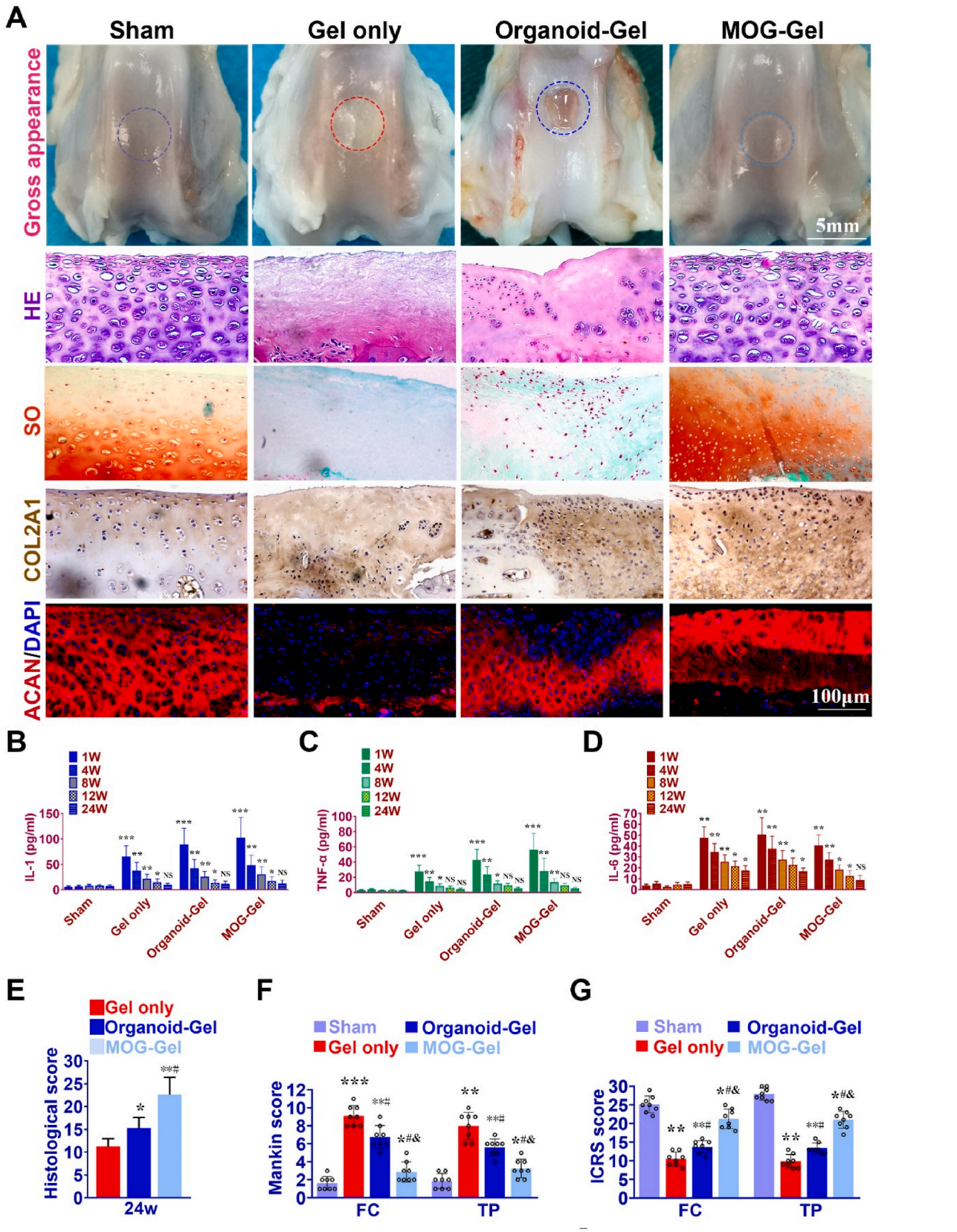

(caption on next page)

Fig. 6. MSOH repaired Cartilage defect and protected long-term joint function in vivo.
A Histological assessment of joint cartilage with HE (2nd row), safranin-O (3rd row), immunohistochemical staining for collagen II (4th row) and immunofluorescent staining for ACAN (5th row. red, ACAN; blue, DAPI) in different groups.
B Examination of intra-articular inflammatory response in the joint fluid was conducted with quantification of IL-1 concentration using ELISA kit. *p < 0.05,**p < 0.01, ***p < 0.001 and NS not significant compared to sham group at the correspondent time point.
C Examination of intra-articular inflammatory response in the joint fluid was conducted with quantification of TNF-α concentration using ELISA kit. *p < 0.05,**p < 0.01, ***p < 0.001 and NS not significant compared to sham group at the correspondent time point.
D Examination of intra-articular inflammatory response in the joint fluid was conducted with quantification of IL-6 concentration using ELISA kit. *p < 0.05,**p < 0.01, ***p < 0.001 and NS not significant compared to sham group at the correspondent time point.
E Histological grading of repaired cartilage in different groups over 24 weeks. *P < 0.05, **p < 0.01 compared to the Gel only group, #p < 0.05 compared to the Organoid-Gel group.
F Articular cartilage in organoid-gel and MOG-gel groups showed declined Mankin scores and G higher ICRS histological score compared to the sham and gel-only group in the femoral condyle (FC) and tibial plateau (TP) over the 24 weeks in vivo.
F Mankin histological score of articular cartilage in the femoral condyle (FC) and tibial plateau (TP) in different groups with scaffold implantation compared to the native cartilage with no implantation surgery. *P < 0.05, **p < 0.01 and ***p < 0.001 compared to the Sham group, #p < 0.05 compared to the Organoid-Gel group, &P < 0.05 compared to the Gel-only group.
G ICRS histological score of articular cartilage in the femoral condyle (FC) and tibial plateau (TP) in different groups with scaffold implantation compared to the native cartilage with no implantation surgery. *P < 0.05, **p < 0.01 and ***p < 0.001 compared to the Sham group, #p < 0.05 compared to the Organoid-Gel group, &P < 0.05 compared to the Gel-only group.

cartilage, was observed in the generated cartilage in the MSOH hydrogel group, indicating successful reconstruction of articular cartilage with abundant ECM deposition. The inflammatory markers for intra-articular inflammation were also tested in vivo. Examination of intra-articular inflammatory response in the joint fluid was conducted with quantification of IL-1, TNF-α and IL-6 (Fig. 6B–D). Compared to the sham group, hydrogel implantation in both groups initiated a transient increased during the acute phase post implantation. The concentration of IL-1, TNF-α and IL-6 in three hydrogel group began toi declined at four weeks and maintained at relatively low level during the 24 weeks of cartilage repair process. No statistically significant difference was observed for the three groups with hydrogel at 24 weeks compared to the sham group. Histological grade of the repaired cartilage demonstrated better repairing effects of MSOH hydrogel compared to the hydrogel in the control groups over 24 weeks (Fig. 6E). However, articular cartilage in all groups with hydrogel implantation showed elevated Mankin histological score compared to the native cartilage with no implantation surgery (Fig. 6F). But the ICRS score declined in all groups with hydrogel implantation (Fig. 6G). Compared to the control group, the MSOH hydrogel showed better chondroprotective effects with a significantly lower histological grading in the femoral condyle (FC) and tibial plateau (TP) over the 24 weeks in vivo. In summary, these results indicated that, compared to the hydrogel with only gel or SMSCs loaded, the MSOH hydrogel not only showed better cartilage repairing effects, but better maintained joint function with low intra-articular inflammatory response after transplantation.

2.7. Implanted MSOH repaired cartilage defect and reversed cellular senescence by regulating miR-24/TAOK1 signaling axis

To further investigate the chondrogenic potential of MSOH hydrogel, mRNA profiles of cartilage sample with MSOH hydrogel and gel only hydrogel were comparatively analyzed with mRNA sequencing (Fig. 7A). Differentially regulated mRNAs were significantly upregulated. Volcano plot revealed difference of transcription in MSOH hydrogel group and gel only hydrogel group (Fig. 7B). All differentially expressed genes were subjected to gene ontology (GO) analysis (Fig. 7C). GO terms for biological process, molecular function, and cellular component were related to regulation of cell population proliferation, extracellular region part, extracellular matrix, glycosaminoglycan binding and extracellular matrix binding. KEGG Pathway analysis based on the differentially expressed genes was conducted and showed closely associated with microRNAs in cancer, TNF signaling pathway, dilated cardiomyopathy, cellular senescence, PI3K-Akt signaling pathway, IL-17 signaling pathway and age-race signaling pathway (Fig. 7D). Cellular senescence was also enriched in the results of KEGG analysis with predicted target genes. Previous studies have indicated the significance of the cellular senescence in cartilage defects and chondrogenesis. We chose to evaluate senescence, chondrogenesis and inflammatory in MSOH hydrogel mediated chondrogenesis with qRT-PCR (Fig. 7E). MSOH hydrogel decreased cellular senescence and inflammatory compared to the gel only group. Meanwhile, miR-24 MSOH SMSC hydrogel enhanced chondrogenesis by elevating the expression of chondrogenesis-related genes. Immunofluorescence staining showed that cartilage tissue after MSOH hydrogel implantation had abundant HMGB1 and significant lower p16ink4a expression (Fig. 7F). Fluorescent in situ hybridization (FISH) of miR-24 in different groups also confirmed the chondrogenesis effects companied with upregulation of miR-24 expression (Fig. 7F). To further analyze the senescence state of the generated chondrocytes, SA-β-Gal staining was performed for collected chondrocytes in vitro, showing lower percent of SA-β-Gal positive generated chondrocytes after MSOH hydrogel implantation (Fig. 7I and J). As for senescence markers HMGB1 and p16INK4a were further validated with qRT-PCR, confirming MSOH mitigated the inflammatory environment and senescence state of generated chondrocytes (Fig. 7G and H). Fluorescent in situ hybridization (FISH) of miR-24 in different groups also confirmed upregulation of miR-24 in neo-formed chondrocytes for MSOH (Fig. 7K). These results indicated that MSOH hydrogel exerted chondrogenic effects by inhibiting cellular senescence through the enriched miR-24/TAOK1 signaling axis.

2.8. MSOH-derived cartilage demonstrated better chondrocyte homeostasis to alleviate cellular senescence and joint degeneration in single-cell transcriptomic analysis

To explore the underlying anti-osteoarthritic mechanism of MSOH-derived chondrocytes, we generated scRNA-seq profiles for the neo-formed cartilage of the gel only group and the MOG gel group (Fig. 9A). After initial quality control, 15,675 and 17,318 cells were acquired for the analysis of single-cell transcriptomes in gel only MOG gel groups respectively (Fig. 8A). Based on the principle component analysis on gene expression patterns, 15 main clusters of cells with specific gene expression profiles were identified (Fig. 8A–D). In most cases, the well-known gene markers were used to identify specific cell types, such as SOX9, ACAN, COL2A1 and COMP for chondrocytes [21,22], COL1A1 and COL1A2 for osteoblasts [22,23] (Fig. 8E–G).Based on t-SNE analysis, unbiased clustering of the cells parallelly identified four main chondrocyte clusters according to their gene profiles and canonical markers (Fig. 8A–C). Particularly, these cell clusters were: (C1) the homeostatic chondrocytes (HomCs) highly expressing PITX1, CHI3L1, SLC26A4 [21,24]; (C5) the proliferative chondrocytes (ProCs) preferentially expressing KCND2, DKK1 and S100A1 [25]; (C7) the Regulatory chondrocytes (RegCs) specifically expressing LAMA2, PIEZO2, COL6A3 [26]; (C10) the Degenerative chondrocytes (DegCs) with high

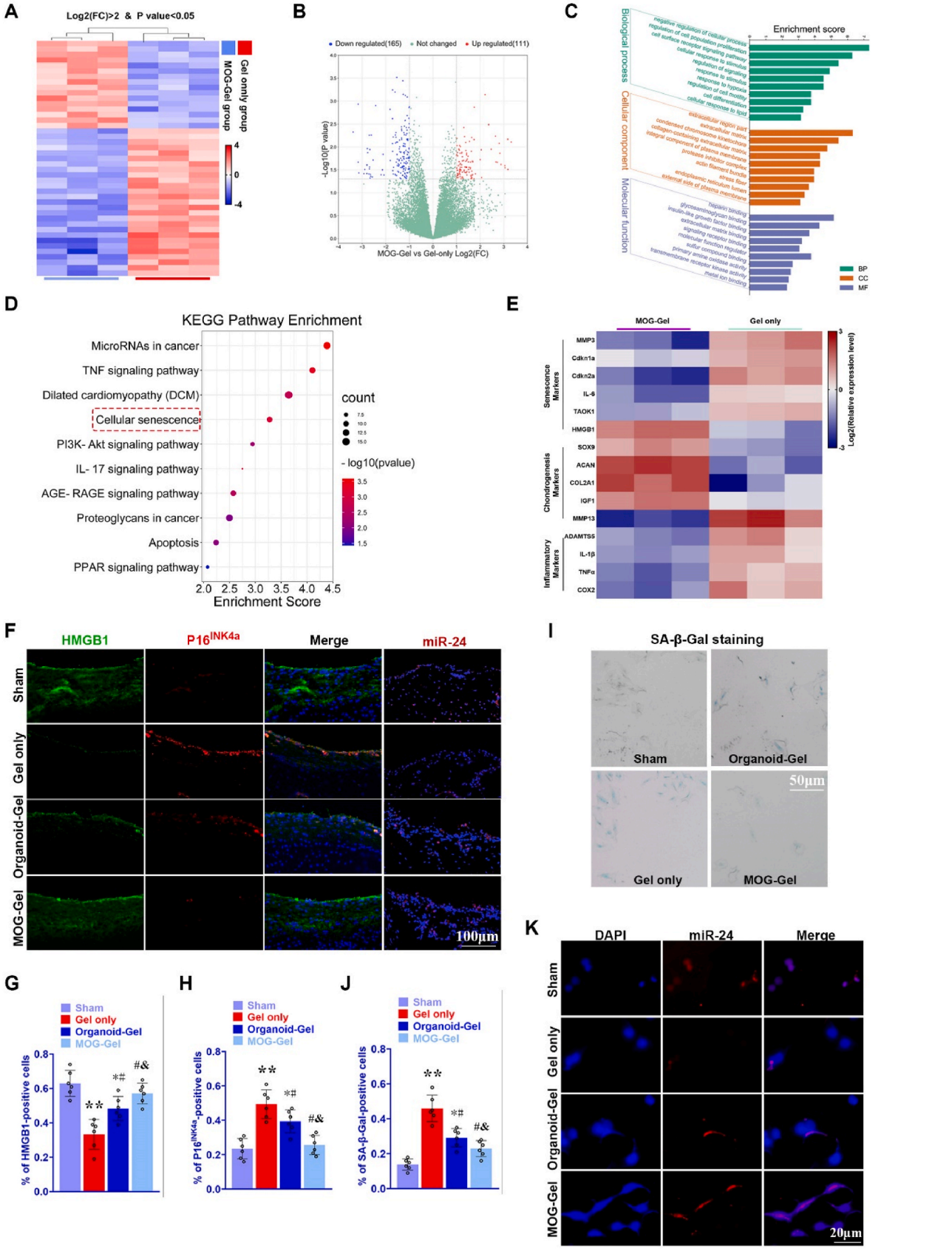

(caption on next page)

Fig. 7. Implanted MSOH repaired cartilage defect and reversed cellular senescence by regulating miR-24/TAOK1 signaling axis
A Heatmap of clustering gene expression profiles with microarray in gel-only group compared to MOG-Gel group. (n = 3 for each group)
B Volcano plot of RNA expression profiles of MOG-gel group and gel-only group.
C Significantly enriched pathways for MOG-gel group in Gene Ontology (GO) pathways.
D Significantly enriched pathways for MOG-gel group in Kyoto Encyclopedia of Genes and Genomes (KEGG) pathways.
E Heatmap of clustering gene expression profiles with q-PCR in MOG-gel group and gel-only group. (n = 3 for each)
F Immunofluorescence staining of HMGB1, P16INK4a and miR-24 (FISH) of cartilage tissue in different groups. (green, HMGB1; red, p16INK4a; blue, DAPI; pink, miR-24)
G Percent of HMGB1 positive cell in cartilage sample from different groups. (n = 6 for each) *P < 0.05, **p < 0.01 compared to the Sham group, #p < 0.05 compared to the Organoid-Gel group, &P < 0.05 compared to the Gel-only group.
H Percent of p16INK4a positive cell in cartilage sample from different groups. (n = 6 for each)
I SA-β-Gal staining of cartilage sample from different groups. *P < 0.05, **p < 0.01 compared to the Sham group, #p < 0.05 compared to the Organoid-Gel group, &P < 0.05 compared to the Gel-only group.
J Percent of SA-β-Gal positive cell in cartilage sample from different groups. (n = 6 for each)
K fluorescent in situ hybridization (FISH) of miR-24 in cartilage tissue from different groups. (red, miR-24; blue, DAPI) *P < 0.05, **p < 0.01 compared to the Sham group, #p < 0.05 compared to the Organoid-Gel group, &P < 0.05 compared to the Gel-only group.

expression of CLEC3A, CAMP and PLA2G2A (*22*). We noticed that, in Gel only cartilage, the frequency of HomCs was significantly declined (Fig. 8B–D). MOG gel caritlage demonstrated higher proportions of ProCs and RegCs, while the frequency of DegCs was remarkably increased in Gel only cartilage (Fig. 8D), indicating loss of cartilage homeostasis and severe joint degeneration in Gel only cartilage. Moreover, the varied proportion of the four chondrocyte clusters between the two samples suggests high heterogeneity of regenerated chondrocytes (Fig. 8D). To further understand the difference between the cartilage samples from gel only and MOG gel group, gene expression data were analyzed by KEGG analysis (Fig. 8G and H). KEGG analysis indicated that Gel only and MOG gel group demonstrated significantly high similarity in enriched pathways, both resulting in the differential expression of genes involved in TGFβ signaling pathway, Longevity regulating pathway, Apoptosis, FOXO signaling pathway, Signaling pathways regulating pluripotency of stem cells, Cellular senescence and HIF-1 signaling pathway (Fig. 8H). Gene set enrichment analysis (GSEA) further verified enriched pathways related to Apoptosis, Cell cycle and Wnt signaling pathway in Gel only group (Fig. 8I–K), while TGFβ signaling pathway, Glycolysis and Oxidative phosphorylation (OXPHOS) was significantly enriched in MOG gel group (Fig. 8L-N), implying that the MOG gel would alter the chondrocyte cellular state by regulating these mentioned pathways above, alleviating chondrocyte senescence and mitigating cartilage and joint degeneration.

Since different chondrocytes may acquire unequal features, we further re-clustered chondrocytes into seven subclusters (Fig. 9A). Higher proportions of subcluster C1 to C5 was identified in MOG gel group, while C6 and C7 subcluster was significantly enriched in Gel only group (Fig. 9B and C). In chondrocytes, GSEA analysis further verified enriched pathways related to Apoptosis, Wnt signaling pathway and PPAR signaling pathway in Gel only group (Fig. 9D–F). In comparison, genes involved in Glutathione metabolism, Glycolysis and OXPHOS were significantly enriched in MOG Gel group (Fig. 9G–I). Among the seven subclusters, C6 and C7 were identified as senescent and degenerative clusters with expressed genes highly enriched in Cell senescence and autophagy (Fig. 9J and K). C1 was identified as homeostatic cluster with high expression of genes encoding proteins involved in Circadian rhythm and FOXO signaling pathway (Fig. 9J and K). C2 was regulatory cluster with specifically expressed genes related to mitophagy and OXPHOS (Fig. 9K). C3 was identified as an effector chondrocyte cluster with expressed genes enriched in Cell cycle, ECM-receptor interaction and PI3K-Akt signaling pathway. Furthermore, C4 was identified as an oxidative stress cluster because of preferentially expressed genes related to OXPHOS and Ferroptosis (Fig. 9K). C5 was identified as a metabolic cluster with expressed genes involved in HIF1 signaling pathway and Metabolic pathways. GSEA also confirmed the characteristics of these seven subclusters (Fig. 9K). Altogether these results provided the mechanism evidence for MOG gel in mitigating chondrocyte senescence and joint degeneration in vitro and in vivo from the perspective of single-cell transcriptome, which addressed that the MSOH could affect chondrocyte homeostatic state and alter the chondrocyte cluster frequency by regulating cellular glycolysis and OXPHOS, impacting cell cycle and ferroptosis to alleviate cellular senescence and prevent joint degeneration.

3. Discussion

In our present study, we have demonstrated that senescence makers are closely correlated with CD in osteoarthritic patients. Reduction of miR-24 expression was identified and served as a senescent marker for cellular senescence in osteoarthritic CD patients. Specifically, chondrocyte cellular senescence was induced in vitro with H2O2 treatment. Consequently, miR-24 expression was remarkably reduced in H2O2-treated experimental SMSC and SMSC organoids. Moreover, targeting senescence with miR-24 overexpression was capable of suppressing cellular senescence and inflammation by inhibiting TAOK1. As a result, we fabricated senescence-targeted miRNA-24/SMSC organoid composite hydrogel (MSOH) accordingly and proved its therapeutic effects in repairing cartilage in osteoarthritic microenvironment, alleviating joint degeneration, as well as promoting regenerative capability and maintaining the homeostatic state of chondrocyte and cartilage by regulating cellular senescence.

The potential applications of SMSCs for cartilage regeneration and OA treatment have been widely studied in the past. SMSCs could enhance adipogenic and chondrogenic differentiation while bone marrow preferentially differentiated into bone [27]. This characterization makes SMSCs an ideal source of cellular treatment for cartilage defects. SMSC organoids are derived with great ability of self-organization [28,29]. SMSC organoids serve as a source of transplantable tissues with functional cell types for CD and osteoarthritis therapy [30,31]. Meanwhile, SMSC organoids can act as the carrier of genetic modification due to their self-renew ability and self-attain characterization [28,32]. Bioengineering strategies could enhance the characterization of these organoids, promote maturations and increase the complexity of the transplanted tissues [28]. Our previous studies indicated that miRNA priming of SMSCs could generate hyaline cartilage in articular surface. Present findings further demonstrated that miRNA microspheres primed with SMSC organoids could serve as a capable and effective means to generate cartilage and suppress cellular senescence in osteoarthritic microenvironment in vivo [20]. Our current study focused on the therapeutic effects of hydrogel-embedded and microRNA-modified SMSC organoids and demonstrated the competence of anti-senescence and pro-chondrogenic function in cartilage repair and osteoarthritis treatment. The composite hydrogel showed slow degradation after implantation, providing good structural integrity for the focal repaired cartilage and mechanic support in weight bearing as the scaffold degrades.

MicroRNA, known as its role in partial complementarity to target

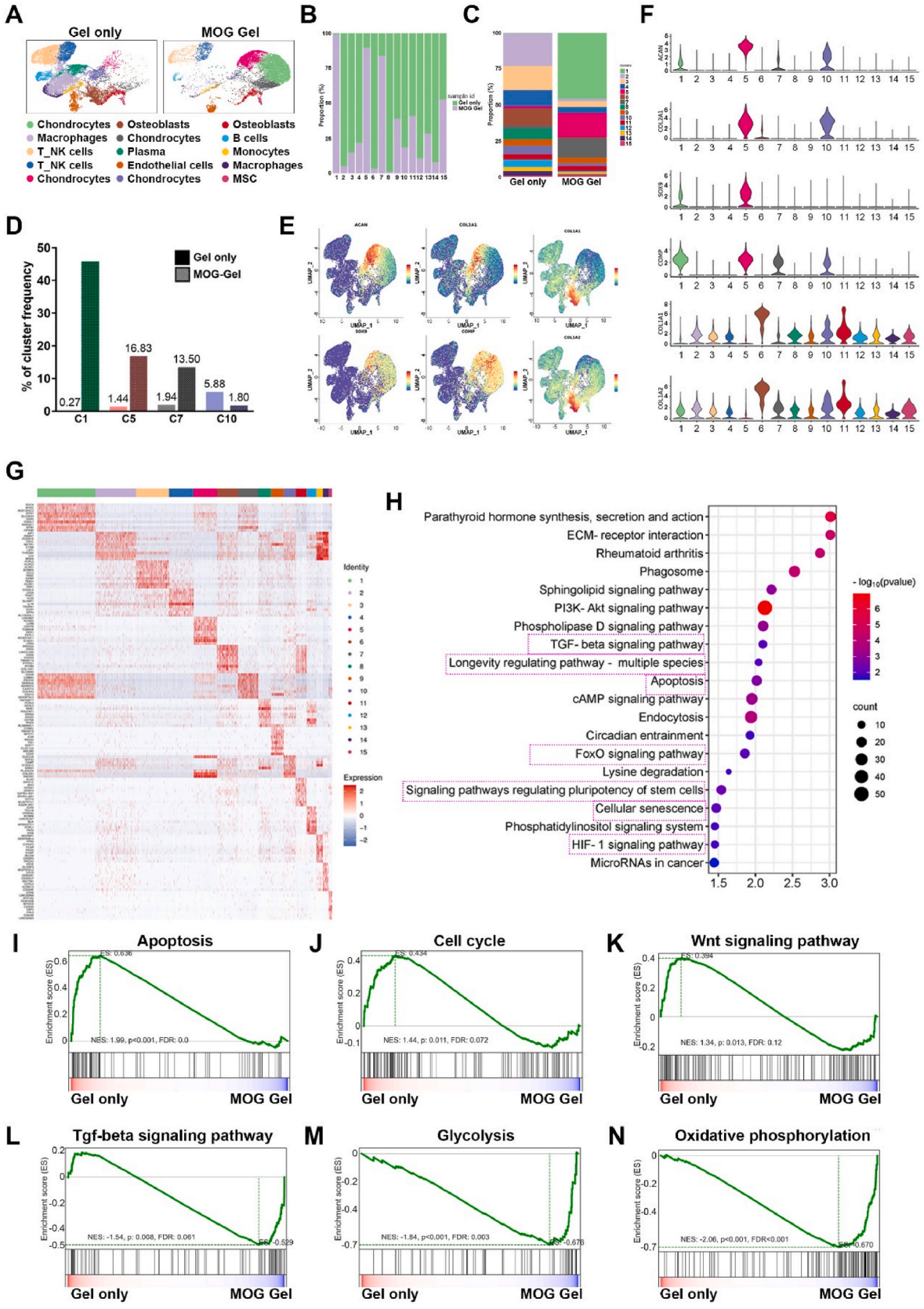

(caption on next page)

Fig. 8. Single-cell transcriptomic analysis of MOG Gel-derived cartilage compared to Gel only-derived cartilage.
A. The t-distributed stochastic neighbor embedding (t-SNE) plot of the five identified main chondrocyte clusters in Gel only-derived and MOG Gel-derived cartilage samples.
B. Relative proportion of each cluster across three cartilage samples as indicated.
C. The frequency of each cluster in the Gel only -derived and MOG Gel-derived cartilages.
D. Frequency of each of five chondrocyte clusters in the Gel only -derived and MOG Gel-derived cartilages.
E. tSNE plots of the expression levels of chondrocyte marker genes (ACAN, SOX9, COL2A1 and COMP)and osteoblast marker genes (COL1A1 and COL1A2).
F. Violin plots demonstrating the normalized gene expression levels of preferentially expressed and representative chondrogenic and osteoblastic marker genes among the 15 clusters.
G. Heatmap revealing the scaled expression of preferentially and differentially expressed genes for each cluster.
H. The Kyoto Encyclopedia of Genes and Genomes (KEGG) enrichment analysis showing differentially enriched signaling pathways in MOG Gel-derived cartilage compared to Gel only-derived cartilage. The representative pathway terms were marked with frames of red dotted line.
I–N. Gene set enrichment analysis (GSEA) revealing the enrichment of representative function terms in OG Gel-derived cartilage compared to Gel only-derived cartilage. NES, normalized enrichment score; P, P value.

mRNA, and its regulation of gene expression at the post-transcription level, is pivotal of modulating biological process including homeostasis and senescence [9,26–30]. As with osteoarthritis, its progression has been reported to associate with deregulation of microRNAs targeting senescence, matrix degrading enzyme, proinflammation cytokines etc [33,34]. For miR-24, its reduction is identified with cellular senescence, and miR-24 overexpression inhibits mitochondrial ROS generation and DNA impair [34,35]. Furthermore, miR-24 might affect cellular senescence and matrix remodeling in OA via regulating p16INK4a according to previous research [35]. Particularly in our study, we elucidated the significance of miR-24 in regulating cellular senescence and chondrogenesis in osteoarthritic microenvironment. Chondrocytes in degenerative joint cartilage might release pro-inflammatory cytokines and thus lead to premature chondrocytes senescence. However, our study proves that miR-24 mimics in SMSC could reverse the senescent trend and significantly regulated the expression of senescence marker HMGB1 and $P16^{INK4a}$ by targeting downstream TAOK1. However, nucleic acids are large, negatively charged molecules and targeted by many endogenous nucleases. In this case, many protective vectors have been explored for miRNA mimics delivery, including PLGA nanoparticles. Based on previous studies, microRNA PLGA microspheres not only avoid limitations with viral vectors (e.g. carcinogenesis [36], immunogenicity [37], broad tropism [38], difficulty of protection [39], but also have good prediction of off-target effects via bioinformatic analysis [40]. Considering such merits, miR-24 mimics were transferred into SMSC organoids by the form of PLGA microsphere in our research. PLGA microsphere-encapsulated miR-24 mimics facilitate intracellular delivery, enhance in vivo stability and target the delivery of the miR-24 mimics. PLGA microsphere offers the advantage of an increased miRNA circulation half-life to obtain a sustained and controlled release. Moreover, fabricated composite hydrogel is able to provide stable microenvironment for organoids development and further enhances the organoids architecture [28]. That's why we used miR-24 mimics microsphere-contained organoid hydrogel to conduct in vivo experiments. Senescence-targeted MSOH gel with the combination of SMSC organoid and miR-24 mimics microspheres would therefore provide new therapeutic options for the treatment of cartilage defect in the osteoarthritic states with cellular senescence. The controlled release of PLGA-encapsulated miR-24 mimics would also target the host chondrocytes and delay the senescence state of these cells. Therefore, the fabricated senescence-targeted MSOH hydrogel could be a novel therapy for cartilage repair and joint protection in osteoarthritic CD patients.

Using scRNA-seq profiles for generated chondrocytes of MSOH-derived cartilage, we further demonstrated improved chondrocyte homeostasis to alleviate cellular senescence and joint degeneration from the perspective of single-cell transcriptome. Our results indicated that MSOH could affect chondrocyte homeostatic state and alter chondrocyte cluster frequency by regulating cellular glycolysis and OXPHOS, impacting cell cycle and ferroptosis to alleviate cellular senescence and prevent joint degeneration [41–45]. Glycolysis is the primary metabolic energy source for chondrocytes. Our scRNA-seq results demonstrated that MSOH might combat cellular senescence and exert its chondrogenic properties via reprogramming cellular energy metabolism in generated chondrocytes. Our results demonstrated targeting cellular senescence by boosting miR-24/TAOK1 axis might be of interest to potentiate cellular therapies in cartilage repair and OA treatment. For translation, we envision injectable MSOH hydrogel ready to implant for cartilage repair in osteoarthritic CD patients within a mini-invasive surgery.

This study has several limitations. First, the binding sites of miR-24 and TAOK1 mRNA were predicted based on databases. The regulatory mechanism of miR-24 needs further confirmation via molecular biology studies. Moreover, the SMSC were derived from human beings and may trigger allogenic response by the rat line. The rejections of heterologous organoids transplantation need to be carefully verified in further studies. Also, the carcinogenicity of microsphere and miRNA-modified SMSC required long-term investigation.

In conclusion, Osteoarthritic cartilage defect patients demonstrated upregulated cellular senescence in joint cartilage. Senescence marker miR-24 was negatively associated with cartilage impairment in osteoarthritic CD patients. miR-24 attenuates chondrocytes senescence and promotes chondrogenesis in SMSC organoids through targeting TAOK1. Senescence-targeted miR-24 microsphere/SMSC organoid composite hydrogel could successfully repair cartilage defect in osteoarthritic microenvironment via enhanced miR-24/TAOK1 signaling pathway, suggesting MSOH might be a novel therapy for cartilage repair in osteoarthritic CD patients.

Data and materials availability

All data associated with this study are present in the paper or the supplementary materials.

Ethics approval and consent to participate

All patients agreed to participate in the study and gave consent for publication and animal experiments were approved by the Laboratory Animal Center in Shanghai Ninth People's Hospital affiliated from Shanghai Jiao Tong University School of Medicine.

CRediT authorship contribution statement

Ye Sun: Writing – review & editing, Writing – original draft, Validation, Supervision, Resources, Investigation, Funding acquisition, Formal analysis, Conceptualization. **Yongqing You:** Validation, Formal analysis, Data curation, Conceptualization. **Qiang Wu:** Writing – original draft, Methodology, Investigation, Formal analysis, Data curation. **Rui Hu:** Writing – review & editing, Writing – original draft, Data curation. **Kerong Dai:** Validation, Supervision, Resources, Conceptualization.

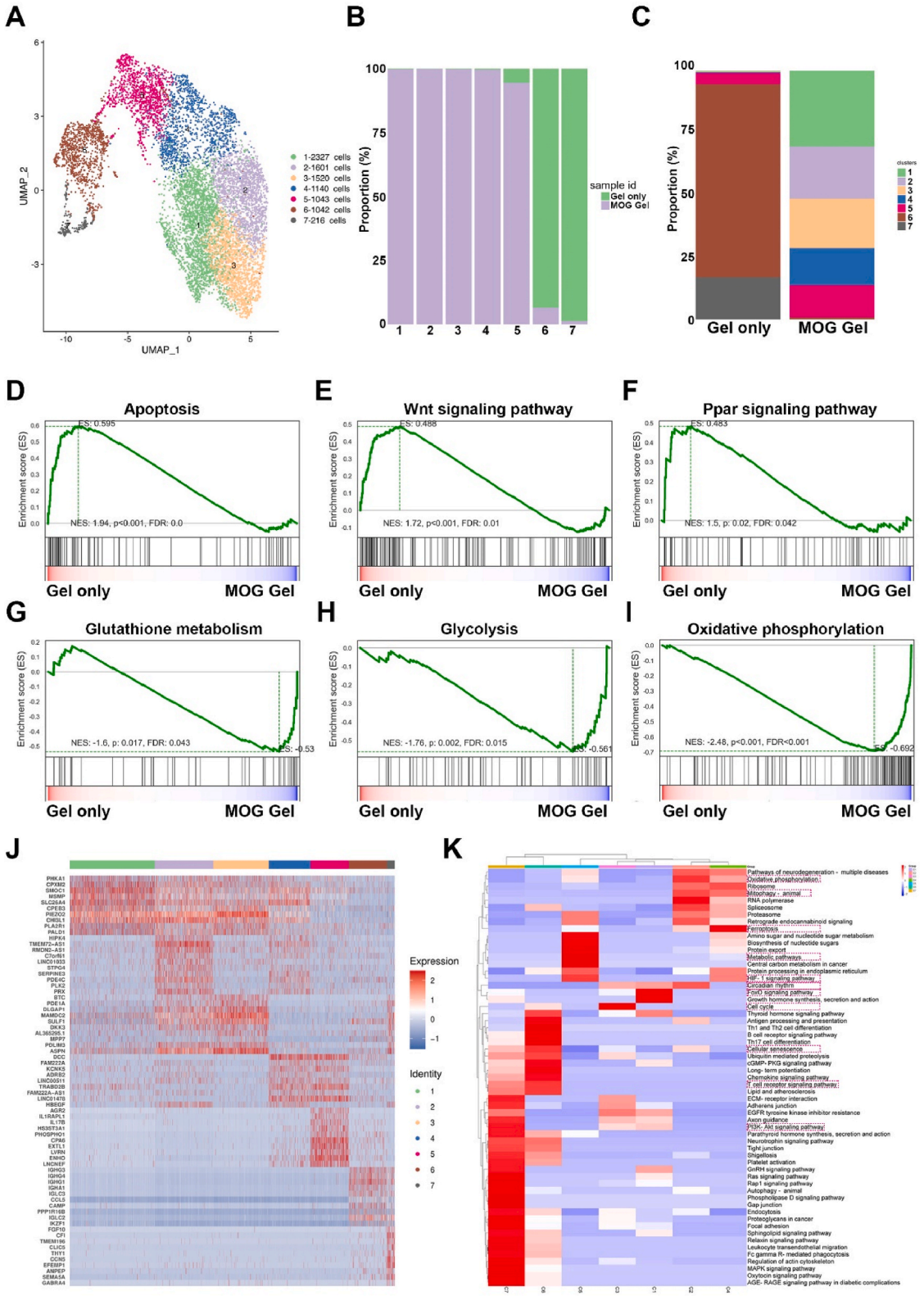

Fig. 9. Transcriptional Heterogeneity of subclustered chondrocytes in MOG Gel-derived cartilage compared to Gel only-derived cartilage.
A. Visualization of t-SNE colored subclusters within chondrocytes in single-cell transcriptomic analysis.
B. Relative proportion of each subcluster across two cartilage samples as indicated.
C. The frequency of each subcluster in the Gel only-derived and MOG Gel-derived cartilages.
D-I. GSEA showing the representative function among each subcluster. NES, normalized enrichment score.
J. Heatmap showing the highly expressed genes in the seven chondrocyte subclusters.
K. The heatmap of Kyoto Encyclopedia of Genes and Genomes (KEGG) analysis showing differentially enriched signaling pathways among the seven chondrocyte subclusters. The representative pathway terms were marked with frames of red dotted line.

Declaration of competing interest

The authors have declared that no competing interest exists.

Acknowledgement

We thank Jie Zhao, Huiwu Li, Yuanqing Mao, Yongyun Chang and Xiaoxiao Yang for their technical help. Funding: This work was funded by the China National Natural Science Funds (No.82172446). We are also grateful for the help and advice from Professor Kerong Dai from Shanghai Ninth People's Hospital, Shanghai Jiaotong University.

Abbreviations

3D	Three-dimensional
miRNA	microRNA
CD	cartilage defects
MSOH	microRNA-24 microsphere/SMSC organoid hydrogel
ELISA	enzyme-linked immunosorbent assay
GAG	glycosaminoglycan
OA	osteoarthritis
OE	overexpress
SMSC	synovial mesenchymal stem cell

Appendix A. Supplementary data

Supplementary data to this article can be found online at https://doi.org/10.1016/j.bioactmat.2024.05.036.

References

[1] L. Sharma, Osteoarthritis year in review 2015: clinical, Osteoarthritis Cartilage 24 (2016) 36–48.
[2] Y. Sun, et al., Chondrogenic primed extracellular vesicles activate miR-455/SOX11/FOXO axis for cartilage regeneration and osteoarthritis treatment, NPJ. Regen. Med. 7 (2022) 53.
[3] C. Parker, et al., Osteochondral allograft transplantation for knee cartilage and osteochondral defects: a review of indications, technique, rehabilitation, and outcomes, JBJS Rev. 7 (6) (2019) e7.
[4] K. Ajay, et al., High tibial osteotomies for the treatment of osteoarthritis of the knee, JBJS Rev. 10 (1) (2022) e21.00127.
[5] J. Jason M, K. Lindsay, B. Michael, Medial unicompartmental arthroplasty of the knee, J. Am. Acad. Orthop. Surg. 27 (5) (2019) 166–176.
[6] T. Wang, et al., Enhanced chondrogenesis from human embryonic stem cells, Stem Cell Res. 39 (2019) 101497.
[7] Q. Wu, et al., Complementary and synergistic effects on osteogenic and angiogenic properties of copper-incorporated silicocarnotite bioceramic: in vitro and in vivo studies, Biomaterials 268 (2021) 120553.
[8] A. Sharafabadi, M. Abdellahi, A. Kazemi, A. Khandan, N. Ozada, A novel and economical route for synthesizing akermanite (CaMgSiO) nano-bioceramic, Mater. Sci. Eng., C 71 (2017) 1072–1078.
[9] A. Najafinezhad, et al., A comparative study on the synthesis mechanism, bioactivity and mechanical properties of three silicate bioceramics, Mater. Sci. Eng., C 72 (2017) 259–267.
[10] J. Meng, C.F. Adkin, V. Arechavala-Gomeza, L. Boldrin, F. Muntoni, J.E. Morgan, The contribution of human synovial stem cells to skeletal muscle regeneration, Neuromuscul. Disord. 20 (1) (2010 Jan) 6–15, https://doi.org/10.1016/j.nmd.2009.11.007.
[11] W. Zheng, Q. Chen, Y. Zhang, R. Xia, X. Gu, Y. Hao, Z. Yu, X. Sun, D. Hu, BMP9 promotes osteogenic differentiation of SMSCs by activating the JNK/Smad2/3 signaling pathway, J. Cell. Biochem. 121 (4) (2020 Apr) 2851–2863, https://doi.org/10.1002/jcb.29519. Epub 2019 Nov 3.
[12] S. Suzuki, et al., Properties and usefulness of aggregates of synovial mesenchymal stem cells as a source for cartilage regeneration, Arthritis Res. Ther. 14 (2012) R136.
[13] K. To, B. Zhang, K. Romain, C. Mak, W. Khan, Synovium-derived mesenchymal stem cell transplantation in cartilage regeneration: a prisma review of in vivo studies, Front. Bioeng. Biotechnol. 7 (2019 Nov 15) 314, https://doi.org/10.3389/fbioe.2019.00314.
[14] K. To, B. Zhang, K. Romain, C. Mak, W. Khan, Synovium-derived mesenchymal stem cell transplantation in cartilage regeneration: a prisma review of in vivo studies, Front. Bioeng. Biotechnol. 7 (2019 Nov 15) 314, https://doi.org/10.3389/fbioe.2019.00314.
[15] N.J. Bernard, Controlling chondrocyte senescence, Nat. Rev. Rheumatol. 15 (2019) 319.
[16] D. Kang, et al., Stress-activated miR-204 governs senescent phenotypes of chondrocytes to promote osteoarthritis development, Sci. Transl. Med. 11 (2019).
[17] O.H. Jeon, et al., Senescence cell-associated extracellular vesicles serve as osteoarthritis disease and therapeutic markers, JCI Insight 4 (2019).
[18] Y. Zhang, et al., Dual functions of microRNA-17 in maintaining cartilage homeostasis and protection against osteoarthritis, Nat. Commun. 13 (2022) 2447.
[19] S. Hu, et al., MicroRNA-455-3p promotes TGF-β signaling and inhibits osteoarthritis development by directly targeting PAK2, Exp. Mol. Med. 51 (2019) 1–13.
[20] Y. Sun, Q. Wu, K. Dai, Y. You, W. Jiang, Generating 3D-cultured organoids for pre-clinical modeling and treatment of degenerative joint disease, Signal Transduct. Targeted Ther. 6 (2021) 380.
[21] T. Matsuzaki, et al., FoxO transcription factors modulate autophagy and proteoglycan 4 in cartilage homeostasis and osteoarthritis, Sci. Transl. Med. 10 (2018).
[22] Q. Ji, et al., Single-cell RNA-seq analysis reveals the progression of human osteoarthritis, Ann. Rheum. Dis. 78 (2019) 100–110.
[23] Y. Chen, et al., A high-resolution route map reveals distinct stages of chondrocyte dedifferentiation for cartilage regeneration, Bone Res. 10 (2022) 38.
[24] U. Kreuser, J. Buchert, A. Haase, W. Richter, S. Diederichs, Initial WNT/beta-Catenin activation enhanced mesoderm commitment, extracellular matrix expression, cell aggregation and cartilage tissue yield from induced pluripotent stem cells, Front. Cell Dev. Biol. 8 (2020) 581331.
[25] D. Kennedy, et al., HSPB1 facilitates ERK-mediated phosphorylation and degradation of BIM to attenuate endoplasmic reticulum stress-induced apoptosis, Cell Death Dis. 8 (2017) e3026.
[26] T. Wei, et al., Analysis of early changes in the articular cartilage transcriptisome in the rat meniscal tear model of osteoarthritis: pathway comparisons with the rat anterior cruciate transection model and with human osteoarthritic cartilage, Osteoarthritis Cartilage 18 (2010) 992–1000.
[27] Y. Ogata, et al., Purified human synovium mesenchymal stem cells as a good resource for cartilage regeneration, PLoS One 10 (2015) e0129096.
[28] G. Rossi, A. Manfrin, M.P. Lutolf, Progress and potential in organoid research, Nat. Rev. Genet. 19 (2018) 671–687.
[29] E. Garreta, et al., Rethinking organoid technology through bioengineering, Nat. Mater. 20 (2021) 145–155.
[30] C. Bock, et al., The organoid cell atlas, Nat. Biotechnol. 39 (2021) 13–17.
[31] A. Kazemi, M. Abdellahi, A. Khajeh-Sharafabadi, A. Khandan, N. Ozada, Study of in vitro bioactivity and mechanical properties of diopside nano-bioceramic synthesized by a facile method using eggshell as raw material, Mater. Sci. Eng., C 71 (2017) 604–610.
[32] S.A. Yi, Y. Zhang, C. Rathnam, T. Pongkulapa, K.B. Lee, Bioengineering approaches for the advanced organoid research, Adv. Mater. 33 (2021) e2007949.
[33] D.P. Bartel, MicroRNAs: target recognition and regulatory functions, Cell 136 (2009) 215–233.
[34] R. Vicente, D. Noël, Y.M. Pers, F. Apparailly, C. Jorgensen, Deregulation and therapeutic potential of microRNAs in arthritic diseases, Nat. Rev. Rheumatol. 12 (2016) 211–220.
[35] D. Philipot, et al., p16INK4a and its regulator miR-24 link senescence and chondrocyte terminal differentiation-associated matrix remodeling in osteoarthritis, Arthritis Res. Ther. 16 (2014) R58.
[36] C. Baum, O. Kustikova, U. Modlich, Z. Li, B. Fehse, Mutagenesis and oncogenesis by chromosomal insertion of gene transfer vectors, Hum. Gene Ther. 17 (2006) 253–263.
[37] N. Bessis, F.J. GarciaCozar, M.C. Boissier, Immune responses to gene therapy vectors: influence on vector function and effector mechanisms, Gene Ther. 11 (Suppl 1) (2004) S10–S17.
[38] R. Waehler, S.J. Russell, D.T. Curiel, Engineering targeted viral vectors for gene therapy, Nat. Rev. Genet. 8 (2007) 573–587.
[39] D. Bouard, D. Alazard-Dany, F.L. Cosset, Viral vectors: from virology to transgene expression, Br. J. Pharmacol. 157 (2009) 153–165.
[40] A. Ambade, et al., Pharmacological inhibition of CCR2/5 signaling prevents and reverses alcohol-induced liver damage, steatosis, and inflammation in mice, Hepatology 69 (2019) 1105–1121.
[41] A. Mobasheri, et al., The role of metabolism in the pathogenesis of osteoarthritis, Nat. Rev. Rheumatol. 13 (2017) 302–311.
[42] M. Arra, et al., LDHA-mediated ROS generation in chondrocytes is a potential therapeutic target for osteoarthritis, Nat. Commun. 11 (2020) 3427.
[43] K. Matsuoka, et al., Metabolic rewiring controlled by c-Fos governs cartilage integrity in osteoarthritis, Ann. Rheum. Dis. (2023) 1227–1239.
[44] X. Wu, X. Fan, R. Crawford, Y. Xiao, I. Prasadam, The metabolic landscape in osteoarthritis, Aging Dis. 13 (2022) 1166–1182.
[45] T. Nishida, S. Kubota, E. Aoyama, M. Takigawa, Impaired glycolytic metabolism causes chondrocyte hypertrophy-like changes via promotion of phospho-Smad1/5/8 translocation into nucleus, Osteoarthritis Cartilage 21 (2013) 700–709.